The Role of Metal Lattice Expansion and Molecular π-Conjugation for the Magnetic Hardening at Cu-Organics Interfaces

Lorena Martín-Olivera,[a] Dmitry G. Shchukin,[a] and Gilberto Teobaldi[a,b,*]

[a] *Stephenson Institute for Renewable Energy, Department of Chemistry, the University of Liverpool, L69 3BX Liverpool, United Kingdom*

[b] *Beijing Computational Science Research Centre, Beijing 100193, China*

ABSTRACT

Magnetic hardening and generation of room-temperature ferromagnetism at the interface between originally non-magnetic transition-metals and π-conjugated organics is understood to be promoted by interplay between interfacial charge-transfer and relaxation-induced distortion of the metal lattice. The relative importance of the two contributions for magnetic hardening of the metal remains unquantified. Here, we disentangle their role via Density Functional Theory simulation of several models of interfaces between Cu and polymers of different steric hindrance, π-conjugation and electron-accepting properties: polyethylene, polyacetylene, polyethylene terephthalate and polyurethane. In the absence of charge-transfer, expansion and compression of the Cu face-centered cubic lattice is computed to lead to magnetic hardening and softening, respectively. Contrary to expectations based on the extent of π-conjugation on the organic and resulting charge-transfer, the computed magnetic hardening is largest for Cu interfaced with polyethylene, and smallest for the Cu-polyacetylene systems as a result of a differently favorable re-hybridization leading to different enhancement of exchange interactions and Density of States at the Fermi level. It thus transpires the neither the presence of molecular π-conjugation nor substantial charge-transfer may be strictly needed for magnetic hardening of Cu-substrates, widening the range of organics of potential interest for enhancement of emergent magnetism at metal-organic interfaces.

1. INTRODUCTION

Electronic hybridization at the interface between metal substrates and organic materials, and the ensuing emergence of electronic states and properties different from the interface constituents, has long attracted the interest of the scientific community.[1-6] Understanding hybridization at metal-organic interfaces holds the key to control and fine-tune the emerging electronic and spin properties (injection, storage and transfer) with potential benefits for the miniaturization and energy-efficiency of sensing, information storage and classical or quantum computing.[1-24]

As recently observed, hybridization between a metal substrate and an organic material can be used also to promote magnetism and ferromagnetic ordering between originally non-magnetic components.[25-32] The phenomenon is appealing because control and enhancement of emergent magnetism between cheap and non-toxic materials such as light transition-metals and organic semiconductors may provide more eco-friendly and sustainable alternatives to conventional magnetic materials and devices.[30-32]

Following earlier generation of molecular-localized magnetism in originally diamagnetic molecular adlayer adsorbed on diamagnetic substrates,[25-29] recent experimental characterization of the interfaces between paramagnetic (Sc, Mn, Pt) or diamagnetic (Cu) transition-metal layers and differently π-conjugated organic substrates (fullerene C_{60} and amorphous carbon, **aC**, films of different density) has provided evidence of a second type of emergent magnetism, with room-temperature ferromagnetic ordering being mostly localized either on the metal substrate[30] or at the intimate metal-organic interface.[31] The compelling experimental evidence on the emergence of ferromagnetic ordering has been complemented by Density Functional Theory (**DFT**) modelling of some of the interfaces considered. The available DFT modelling points to both charge-transfer between the metal and the organics, and interface-relaxation induced distortions at the metal substrates as the two key drivers for the magnetic hardening of the metal substrate and consequent emergence of magnetic ordering.[31] To date, the relative importance of charge-transfer between the

metal and (π-conjugated) organic, and distortion of the metal lattice for the emergence of interfacial magnetic ordering remains unquantified, with the immediate consequence of interfaces between metal and non π-conjugated molecules having being overlooked in recent investigations of emergent magnetism.[30-32]

However, recent spin-resolved photoemission spectroscopy measurements on a linear alkane, pentacontane $C_{50}H_{102}$, on Co(001) have unambiguously shown that π-conjugation on the organic is not necessary for emergence of strongly spin-polarized interface states between ferromagnetic metals such as Co and an adsorbed organic molecule or layer.[20] These results inevitably rise the question as to whether π-conjugation is actually necessary (or not) also for the magnetic hardening and emergence of magnetism at the interface between originally non-magnetic transition metals and molecular systems.

To answer this question, in this work we disentangle the role of metal distortion, metal-organics charge-transfer, and organic π-conjugation for the magnetic hardening at metal-organic interfaces. Specifically, we screen via DFT the electronic and magnetic properties of several models of interfaces between Cu (known to originate ferromagnetic ordering when contacted with C_{60} and aC films[30-31]) and four polymeric systems of different steric hindrance, π-conjugation and electron-accepting properties, disentangling the relative importance and interplay between these factors and the resultant interface magnetic hardening or softening.

2. METHODS

2.1 Computational details

Following Refs. [30-31], standard and fixed spin-moment,[33] van der Waals (vdW) corrected,[34] Density Functional Theory (DFT) simulations were executed via the Projected Augmented Wave (PAW) method as implemented in the VASP program[35] with the PBE exchange-correlation (XC)

functional,[36] a 400 eV plane-wave energy cut-off, and (0.2 eV, 1st order) Methfessel-Paxton electronic smearing.[37] The grids for **k**-point sampling were defined on the basis of convergence tests on the magnetic properties of bulk Cu in the face-centered cubic (**FCC**) structure (see Figure S1 in the Supporting Information) and scaled according to the size of the reciprocal lattice of the system under consideration. The atomic-force threshold for geometry optimization was 0.02 eV $Å^{-1}$. All the atoms in the Cu slabs and in the polymers were fully relaxed in all the directions. A vacuum separation of at least 15 Å was present between replicated images of the 5-layer Cu(111) slab models for the in-plane interface models (Figure 1). Bader charge analyses[38] were computed on the total charge density i.e. accounting for both the electronic and ionic core charges.

Due to the computed non-magnetic ground-state for all the models studied, atom-resolved approximations to the Stoner exchange integral (I_S) were calculated by enforcing a magnetic moment of 0.1 μ_B/Cu-atom via fixed spin-moment DFT.[33] Following Refs. [39] and [30-31], and owing to the weak wave-vector (**k**) dependence of the energy difference between spin-up and spin-down bands (band-splitting, ΔE),[39] atom-resolved values of I_S were computed from the (PAW-core projected) ΔE values integrated over the Brillouin zone, and the (PAW-core projected) atomic magnetic moment (m) as:

1) $$I_S = \frac{\Delta E}{m}$$

Owing to the dependence of ΔE on the energy of the Kohn-Sham states,[39] the error for the computed I_S was quantified by calculating the standard deviation between the ΔE values at the stationary points (maxima and minima) of the PAW-core projected PDOS in the energy interval between the Fermi energy ($\mathbf{E_F}$) and E_F-3eV. This interval was chosen following numerical tests in order to have at least three stationary points of the PDOS used in the computation of the average I_S value and its standard deviation (see Figure S2 in the Supporting Information). Following Refs. [11, 13, 30-31], increase (decrease) of I_S with respect to the reference bulk value is taken as indication of *magnetic hardening* (*softening*) for a given substrate.

Being based on a mean-field approximation to exchange interactions (as approximately parameterized in the adopted semilocal PBE XC-functional) the procedure cannot intrinsically account for spin-fluctuations that may be responsible for the measured ferromagnetic ordering at the interfaces between originally non-magnetic systems.[30-32] Quantitative description of these effects would require more sophisticated (and computationally demanding) methods capable of describing dynamical aspects of local magnetic susceptibilities.[23, 40-41] In spite of these intrinsic limitations, the approach is nevertheless capable of producing trends in magnetic hardening that semi-quantitatively match the measured magnetization of Cu-C_{60} and Cu-aC interfaces.[30-31] These consideration, and the overall very light computational cost of the approach, enabling fast and convenient simulation of systems up to over 200 atoms as considered in this study, in our view justify its use for exploratory screening of novel strategies towards molecule-induced magnetic hardening and possible emergent magnetism.

Magneto-crystalline anisotropy Energies (MAEs) were computed via fixed-spin moment (0.1 μ_B/Cu-atom), non-collinear DFT simulations with inclusion of spin-orbit coupling as available in VASP.[35] The simulations were carried out non-self-consistently, that is, keeping the charge density (from a collinear run) fixed. The magnetic field was selectively oriented perpendicularly to the high-symmetry directions of the considered system and the corresponding energy subtracted to quantify the MAEs. These non-collinear DFT simulations were performed with the same number of symmetry irreducible **k**-points tested to yield PAW-integrated I_S values (Figure S1 in the Supporting Information and Section 3.1 below) and total DFT energies converged to within 2 meV and <1 meV, respectively for bulk FCC Cu. After the scaling due to the larger simulation cell for the Cu- polyethylene models (Section 3.1), this accounts for 8,436 and 25 (symmetry irreducible) **k**-points for bulk FCC Cu and the Cu-polyethylene interfaces, respectively.

2.2 Interface models

To disentangle the role of Cu-lattice expansion and charge-depletion for the observed magnetic hardening of Cu at molecular interfaces,[30-31] we study several models of interfaces between FCC Cu and organic systems with different electron-accepting properties, steric hindrance or excluded volume and, owing to a different extent of π-conjugation, conformational flexibility and relaxation possibilities when interfaced with the Cu-substrate. We focus on four different polymeric systems, namely polyethylene **(PE)**, polyacetylene **(PAC)**, polyethylene terephthalate **(PET)** and polyurethane **(PUR)**, whose monomeric units are shown in Figure 1. These systems have been chosen on the basis of their different electron affinities (**EA**), thence expected electron-accepting properties neglecting interface-relaxation effects to be quantified in the following. The measured or computed EA for the considered systems range from negative for PE (experimentally derived value: -0.5±0.5 eV[42-46]) to increasingly positive values going from PUR (B3LYP computed vertical value, neglecting electronic and atomic relaxation: 0.63 eV[47]) to PET (experimental value: 2.85±0.05 eV[48]) and PAC (extrapolated –adiabatic- value for infinite chain at B3LYP level: 5.5 eV[49]). Based on these values, the expectation, to be verified against the results for the relaxed interface models, is that the charge-transfer from Cu to the polymer should increase following the series PE < PUR < PET < PAC.

In addition, the systems examined have different torsional flexibility owing to either the lack (PE) or different extent of π-conjugation (PET ~ PUR< PAC), and different steric hindrance due to the presence (PET and PUR) or absence (PE and PAC) of bulkier phenyl groups. Both these elements are anticipated to affect the relaxation at the interface with Cu, enabling quantification of the role of both the polymer-induced distortion of the Cu lattice and the polymer-relaxation for the emerging magnetic properties at the interfaces.

Before proceeding, we recall that all the Cu-organics interfaces capable of emergent magnetism measured to date have been prepared by alternated magnetron sputtering deposition of Cu (metal)

and organics (C_{60} molecules or C-atoms) films. The sample preparation protocol leads to creation of films with nm-range roughness.[30-31] Since, in principle, alternative routes to preparation of single Cu-organics interfaces could be realized via chemical or electrochemical deposition of Cu on a polymeric-film, practical creation of the Cu-polymer interfaces studied below cannot be excluded a priori, motivating out interest in exploring computationally emergent magnetism at suitably treated interfaces of polymer substrates.

In analogy to the molecular films in Refs. [30-31], ordinary noncrystalline films of the polymers considered are not atomically flat, with roughness in the nm-range[46] or above. Since such molecular roughness would inevitably result in growth of the deposited Cu inside pits of the polymer film or around "self-passivating" protruding polymer loops present at the surfaces of polymer-films,[50] we bracket the possible interface geometries by the two extreme cases shown in Figure 1: in the first one, the polymer chain is placed parallel to the Cu(111) planes of a five-layer slab (in-plane model). In the second one, the polymer chain is perpendicular to the slab plane (perpendicular model).

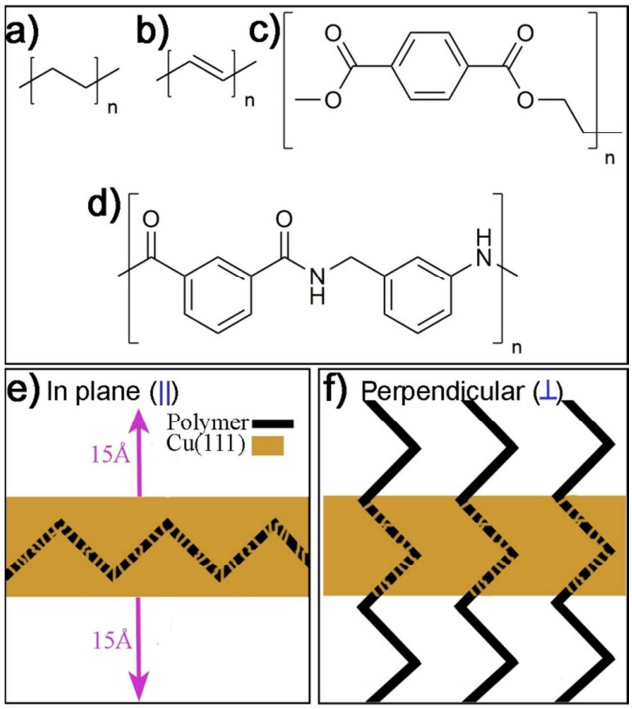

Figure 1. Monomer atomic structure for the polymers considered. **a)** polyethylene **(PE)**, **b)** polyacetylene **(PAC)**, **c)** polyethylene terephthalate **(PET)** and **d)** polyurethane **(PUR)**. Schematic representation of the two interface models used: **e)** in-plane (||) geometry with the polymer chain inserted parallel to the Cu(111) plane, **f)** perpendicular (⊥) geometry with the polymer chain inserted perpendicular to the Cu(111) plane.

Here, it is worth noting that magnetron sputtering preparation of the metal-organic interfaces is *not* a thermodynamic-driven process based on chemical equilibrium. Metastable systems can be initially formed. Indeed, the magnetron-sputtering prepared metal-molecule interfaces are experimentally observed to relax, following thermal treatment or ageing, into lower (free) energy systems of partially or strongly modified magnetic properties.[30-31] These considerations motivate the neglect of thermodynamics-related parameters such as the formation energy (always positive for the considered interface models and progressively less favorable as the number of Cu atoms in the models increases) in favor of an exploratory focus on screening the electronic and magnetic properties of model Cu-polymer interface forcing different degree of interface geometric relaxation.

As in Ref. [30], to include the effects of differently constrained optimization of the Cu-polymer interface on the emerging magnetic properties, different models were prepared for each interface geometry and polymer using several cut-off's on the initial Cu-polymer distance ($d_{Cu\text{-}pol}$=1.5, 2.0, 2.5 and 3.0 Å). The Supporting Information (Figure S3) contains images of a selection of the initial geometries prepared with $d_{Cu\text{-}pol}$=1.5 Å. The value of $d_{Cu\text{-}pol}$ were chosen in order to start the interface structural relaxation both in repulsive and attractive regimes, as estimated from the shortest Cu-C distances measured by I-V LEED for an archetypal interface between Cu and a π-conjugated system: the 7-vacancy C_{60}/Cu(111)-4x4 reconstruction (shortest interfacial Cu-C distance: 1.98 Å, longest interfacial Cu-C distance: 2.20 Å).[51] Since the interface properties depend on the details of the electronic re-hybridization, which may change depending on the relaxation freedom available in the system, this strategy offers the possibility to quantify the role of differently constrained relaxations, as likely present in real samples of limited crystallinity, [30-31] on the emerging electronic and magnetic properties of the models studied.

For the in-plane (||) interface models, commensurability between the Cu(111) slab and the polymer chains was achieved by modelling the smallest Cu(111) slab, in either a hexagonal or orthorhombic cell, capable of minimizing the lattice mismatch with the given periodic polymer chain. Compromising between reduction of the periodicity mismatch and size of the simulation cell, we settled for lattice mismatches <1.2% for PE, PAC and PUR and roughly 3% for PET. The positive lattice mismatch values indicate that the polymer chain was stretched to match the Cu(111) slab one. Table S1 in the Supporting Information reports a summary of the geometric parameters for the simulation cells used for the different Cu-polymer interface models. For the perpendicular (⊥) interface models, the size of the simulation cell along the direction perpendicular to the Cu(111) was based on the optimized period of the given polymer chain.

3. RESULTS AND DISCUSSION

3.1 Magnetic properties of isotropically distorted bulk FCC Cu

With the final aim of disentangling the role of charge-transfer and lattice distortion for the magnetic hardening of Cu, we start our investigation by considering the dependence of the magnetic properties on the local geometry and coordination of Cu atoms in the bulk phase. To quantify the relative importance of both the Cu-Cu distance and coordination symmetry for the magnetic properties of bulk Cu, we focus initially on the effect of isotropic expansion and compression of bulk FCC Cu i.e. distortions altering the Cu-Cu distance without affecting the local coordination symmetry of the Cu atoms.

We first quantify the convergence of the computed atomic magnetic moments (m) and band-splittings (ΔE) (thence I_S in Eq. 1) for bulk Cu in the FCC structure as a function of both the **k**-point grid sampling and the volume of the FCC cell, varied between compressions of 15% and expansion of 20% around the computed energy minimum (3.649 Å lattice parameter, see Figure S1 in the Supporting Information). It is found that a spacing of at least 0.0079 $Å^{-1}$ between **k**-points is sufficiently dense to yield computed values of m, ΔE and I_S converged, over the range of volume changes considered, to within $<10^{-3}$ μ_B, 6 meV and 2 meV, respectively. Based on these results, a spacing of at least 0.0079 $Å^{-1}$ was used for all the simulations of bulk FCC Cu, and the **k**-point sampling for the Cu-polymer interface models was scaled according to the size of the reciprocal lattice to maintain this level of convergence for the magnetic properties.

For the range of volumes considered, the computed PDOS-averaged (see Figure S2 in the Supporting Information) values of I_S for bulk FCC Cu as a function of the lattice parameter (Figure 2a) reveal a small variation (<0.05 eV or, equivalently, <6%) from the optimized reference value. Compression (expansion) of the Cu FCC lattice results in decrease (increase) of I_S, with slightly larger changes (up to 6%, that is 0.05 eV) upon compression. The computed magnetic hardening for expanded Cu lattices agrees qualitatively, but not quantitatively, with results for C_{60}-perturbed FCC

Cu substrates, where increases up to a factor of over three in I_S were computed for 15% expansion of the local Cu FCC coordination.[30] This result provides a first indication that increase of Cu-Cu distances without changes of the local coordination symmetry for Cu-atoms and depletion of the electronic charge by the organics is not exceedingly effective in inducing magnetic hardening of Cu substrates. The similarity between the maximum change of I_S as a function of the volume change (<0.07 eV) and its computed error (up to nearly 0.06 eV for the most deformed cases in Figure 2a) strengthens this conclusion.

However, the increase of I_S with the lattice parameter is accompanied by a parallel rise in the Density of States at the Fermi Energy [DOS(E_F), Figure 2b and 2c], leading to up to 30% larger I_S×DOS(E_F) products (Figure 2d), closer to comply with the Stoner criterion for spontaneous onset of ferromagnetic ordering in *3d* metals (I_S×DOS(E_F) >1.[52-53] Conversely, compression of bulk FCC Cu, and the ensuing reduction in both I_S and DOS(E_F), leads to up to over 30% reduction of I_S×DOS(E_F). These results indicate that volume expansion is more effective than compression in inducing magnetic hardening of bulk FCC Cu. Notably, the largest increase in of I_S×DOS(E_F) for 20% expanded bulk Cu FCC, leading to a value of roughly 0.16 $spin^{-1}$ $atom^{-1}$ is substantially smaller (-30%) than what computed, at the same level of theory, for Cu-C_{60} interfaces (up to 0.23 $spin^{-1}$ $atom^{-1}$),[30] confirming that isotropic FCC expansion may not be the most effective strategy towards magnetic hardening of Cu substrates. However, it also worth noting that for the as prepared Cu-aC interfaces measured to develop ferromagnetic ordering,[31] the computed I_S×DOS(E_F) products are close to 0.15 $spin^{-1}$ $atom^{-1}$, which ultimately points to the exploration of Cu FCC lattice expansion, possibly by epitaxial growth of ultra-thin films on suitable substrates, as a potentially alternative route towards magnetic hardening of Cu and ensuing emergence of ferromagnetic ordering *without* the use of molecular interfaces. This aspect will be the subject of a forthcoming study.

Non-collinear fixed-spin DFT simulations for all the compressed and expanded bulk FCC systems indicate minimal changes (<10^{-7} eV/atom) in the MAEs, that remain consistently in the order of 10^{-6}

eV/atom, in line with the weak shape anisotropies measured for ferromagnetic Cu-C_{60} interfaces (~10^{-6} eV/Cu-atom).[30] Although the computed differences in MAEs are clearly orders of magnitude below the (meV range, see Methods section) convergence of the simulations, the computed MAE-values can be nevertheless taken as an indication that the isotropic deformations studied are not capable of substantially increasing MAEs for Cu-substrates to the meV range, as desirable for practical applications.[13]

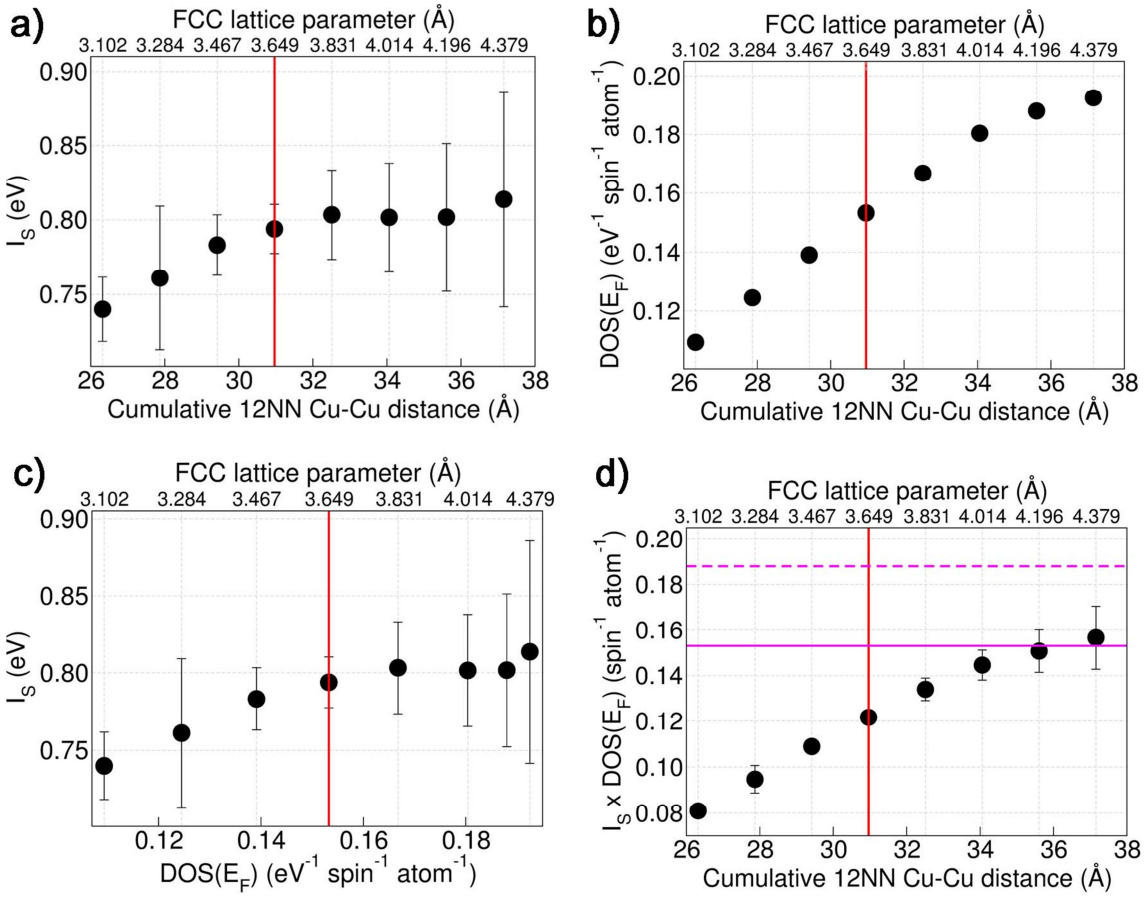

Figure 2. Computed **a)** Stoner exchange integral (I_S), and **b)** Density of States at the Fermi level [$DOS(E_F)$] as a function of both the lattice parameter for bulk FCC Cu and the sum of the 12 shortest nearest-neighbors (NN) Cu-Cu distances. **c)** Computed I_S as a function of $DOS(E_F)$. **d)** Change of $I_S \times DOS(E_F)$ as a function of the lattice parameter. The vertical red line marks the values for the optimized lattice parameter (3.649 Å). The horizontal continuous (0.15 $spin^{-1}$ $atom^{-1}$) and dashed (0.19 $spin^{-1}$ $atom^{-1}$) magenta lines in d) mark the largest computed $I_S \times DOS(E_F)$ product at the same level of theory for the interfaces between Cu and as deposited (1.7 gr/cm^3) and annealed (2.3 gr/cm^3) amorphous carbon measured to be ferromagnetic in Ref. [31].

3.2 Cu-Polymer interfaces

3.2.1 Geometric relaxation of the interface models

Depending on the polymer, and in-plane or perpendicular interface, geometry optimization of the Cu-polymer models (Figure 3) leads to different relaxation of the Cu slab and loosening of the Cu lattice as quantified by the average cumulative 12 nearest-neighbors (**NN)** Cu-Cu distances for the Cu atoms in the slab (Figure 4). In all cases, no barrier-less breaking of the bonds of the polymer chain and atom-transfer to interface Cu-atom during the geometry optimization was observed.

In general, all the interface models considered induce loosening of the FCC Cu lattice. Not unexpectedly, the distortions for the in-plane models are larger than for the perpendicular ones. In line with expectations based on the larger hindrance of the phenyl group (in PUR and PET) with respect to $–CH_2–CH_2–$ (PE) and –CH=CH– (PAC) fragments, the computed loosening of the Cu lattice is largest for PUR and PET. Interestingly, the PAC-induced loosening of the Cu lattice is closer to PUR values than PE results. This result suggests a predominant role of the presence (or absence) of molecular π-conjugation (and ensuing Cu-organics charge-transfer) for the relaxation of the metal substrate. In the following we quantify the extent to which such an enhanced geometric relaxation directly correlates (or not) with the interface electronic and magnetic properties.

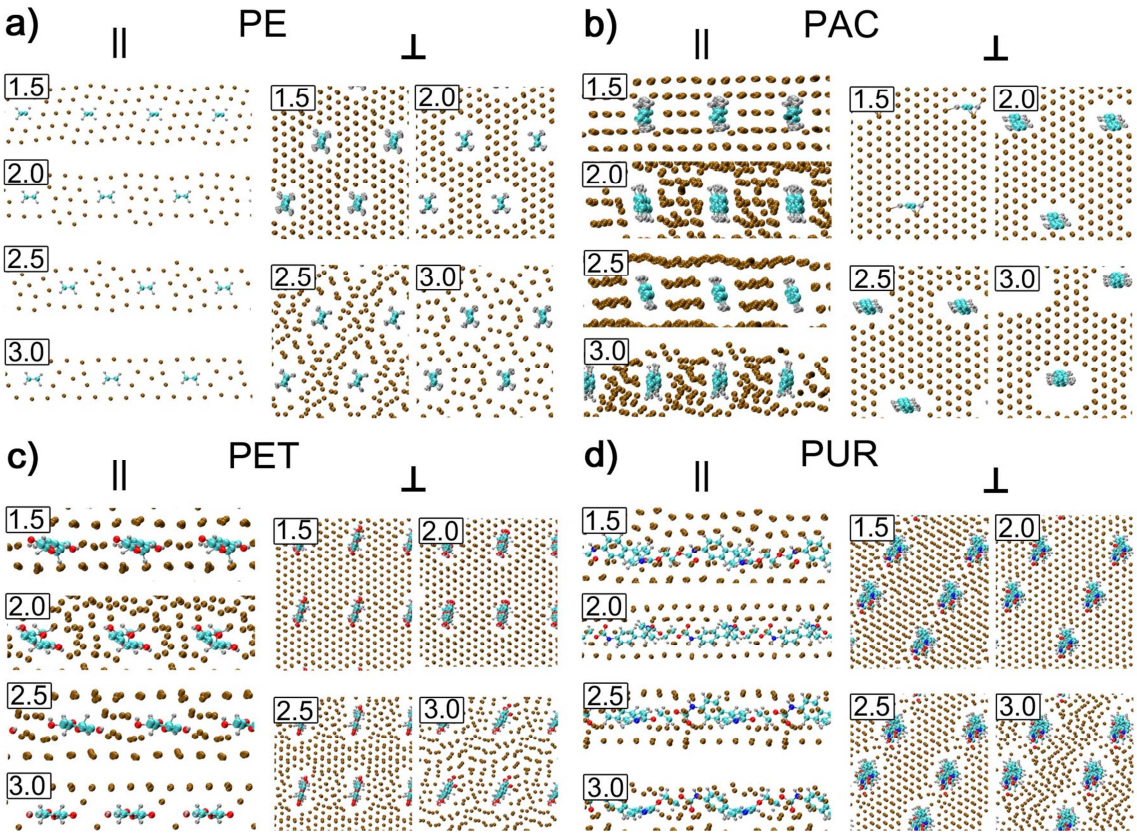

Figure 3. Optimized geometries for the considered in-plane (left sub-panels, side view) and perpendicular (right sub-panels, top view) models of the interface between Cu and **a)** PE, **b)** PAC, **c)** PET, **d)** PUR. The Cu-polymer cut-off ($d_{Cu\text{-}pol}$, Å) used to prepare the initial geometry is reported in the insets. C: cyan, O: red, N: blue, H: silver, Cu: brown.

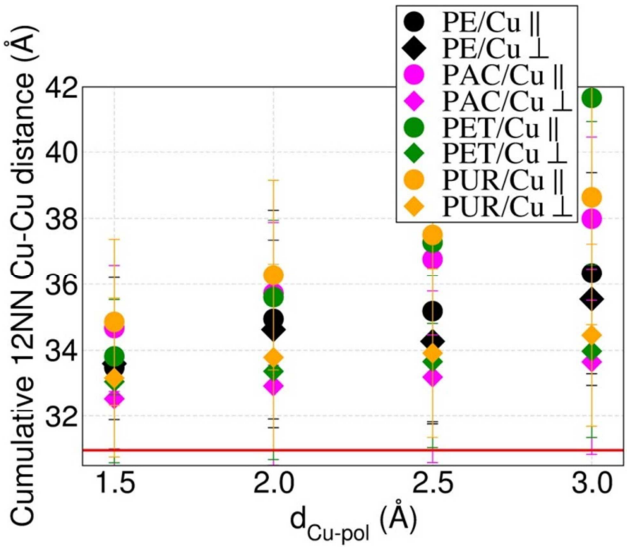

Figure 4. Polymer-induced loosening of the Cu lattice for the Cu-polymer interfaces considered as quantified by the average sum of the 12 NN Cu-Cu distances in the optimized slabs. The horizontal red line marks the value of the cumulative 12 NN Cu-Cu distance (30.962 Å) for optimized bulk FCC Cu (lattice parameter: 3.649 Å).

3.2.2 Electronic properties of the interface models

In spite of the substantial relaxation induced on the Cu-substrate by the polymer chain, all the interfaces are computed to be metallic and characterized by a well-defined *3d* band with an absolute Density of States (DOS) maximum at about 1.5 eV below E_F, as present for bulk FCC Cu (Figure 5). Comparison between Cu and polymer-resolved PAW-projected DOS (PDOS), shown in Figures S4 and S5 in the Supporting Information, indicates that the DOS at E_F [DOS(E_F)] is dominated by Cu states and that the interface relaxation leads to metallization (non-zero PDOS at E_F) for all the polymers. These findings are in qualitative agreement with the results for other interfaces between Cu and differently conjugated systems such as C_{60},[30] aC[31] and linear alkanes,[54] suggesting that π-conjugation of the organics is not necessary for the creation of hybrid Cu-polymer delocalized metallic-states at the interface.

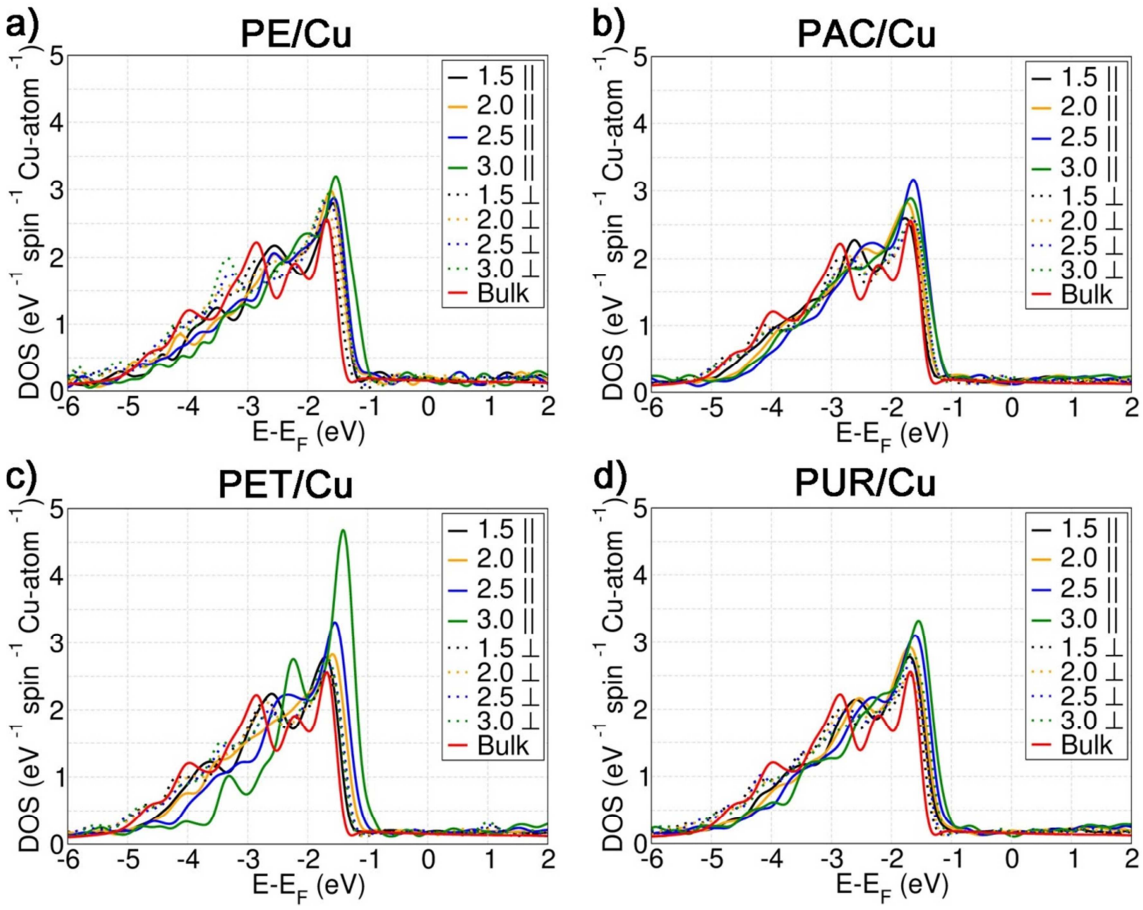

Figure 5. Computed Density of States (DOS) for the in-plane (||, continuous lines) and perpendicular (⊥, dotted lines)) models of the interface between Cu and **a)** PE, **b)** PAC, **c)** PET, **d)** PUR. Black: $d_{Cu\text{-}pol}$=1.5 Å, yellow: $d_{Cu\text{-}pol}$=2.0 Å, blue: $d_{Cu\text{-}pol}$=2.5 Å, green: $d_{Cu\text{-}pol}$=3.0 Å. The computed DOS for bulk FCC Cu at the optimized lattice parameter is shown in red.

Consistent with the larger hybridization between the Cu and polymer modelled for PAC, PET and PUR by comparison to PE, leading to larger polymer-projected PDOS(E_F) for the former systems, (Figure S4 in the Supporting Information), Bader charge analysis for the optimized models reveals a larger Cu→polymer electron transfer for the systems with π-conjugation (PAC, PET and PUR in Figure 6).

Notably, the interfacial charge-transfer turns out to qualitatively correlate with the vertical electron affinity (EA) of the polymer chains, as first approximated by the position of the LUMO for the isolated chain with respect to the vacuum level. With the exception of the in-plane (||) Cu-PUR interface-model prepared with the shortest $d_{Cu\text{-}pol}$ (1.5 Å in Figure 3d), the trend in Bader charge-transfer (PE<PUR<PET<PAC) follows qualitatively what expected on the basis of the vertical EA as first approximated by minus the energy of the LUMO level with respect to the vacuum (again PE<PUR<PET<PAC from Table S2 in the Supporting Information). These results suggest that, at least for the Cu-polymer interfaces studied, trends in interfacial charge-transfer between different molecular systems may be effectively estimated based on the position of the LUMO level for the isolated organic. It consequently follows, again at least for the systems considered, that the different interface relaxation (PE<PAC<PUR~PET in Figure 4) plays a secondary role with respect to the organic EA for the overall interface charge-transfer: larger interface relaxation (Figure 4) does not directly correlate with larger charge-transfer at the interface.

Before proceeding, it is worth nothing that, in spite of the substantial re-hybridization leading to metallization of PE interfaced to Cu, the overall charge-transfer from the Cu substrate to PE in the in-plane models is less than 0.14 e in Figure 6a (0.07 e per PE unit in the simulation cell). This result stems from the competition between Cu→organic donation and organic→Cu back-donation previously discussed for alkanes on metallic substrates such as Cu[54] or Co[20]. Here, it has to be noted that empty (Kohn-Sham) states for PE chains, as typically other saturated aliphatic molecules (alkanes), tend to be localized mostly outside the molecular backbone, leading to accumulation of excess charge in the interstitial regions around the PE chain,[45-46, 55-57] an aspect that may have affected Bader partitioning[38] of the electronic charge at the Cu-PE interfaces.

In line with previous results in the literature,[54] we find that in spite of the minimal net charge-transfer, and the additional constraints induced by the use of infinitely periodic interface models, the Cu-PE re-hybridization and ensuing metallization of the organic system is accompanied by an increase up to 1.5% (decrease up to 4%) of C-H (C-C) bond-distances and a parallel increase up to

3% in the C-C-C bond angles in PE (Table S3 in the Supporting Information). These results are indicative of a partial $sp^3 \rightarrow sp^2$ re-hybridization of the aliphatic chain upon interaction with Cu, as also evident by the dramatic change in PE-resolved DOS for all the Cu-PE interface models (Figure S5 in the Supporting Information).

Finally, analysis of the computed Bader charge-transfer as a function of the loosening of the Cu lattice (Figure 6b) reveals another correlation potentially useful when designing Cu-organic interfaces. For all the interface models considered, the Cu→organic charge-transfer decreases as the local coordination environment of the Cu atoms is expanded. Thus, contrary to the Cu-C_{60} case,[30] increased interface relaxation and loosening of the Cu-lattice is found to hinder, rather than enhance, depletion of electronic charge at the Cu-substrate by the considered organics. This result indirectly suggests that strain on the π-system (larger for C_{60} than the considered, originally planar, PAC, PET and PUR) may play an important role for the interface relaxation and charge-transfer, an aspect worth of detailed investigation in the future. In the following, we quantify to extent to which such a quantitatively different charge-transfer affects the emerging magnetic properties of the Cu-polymer interfaces.

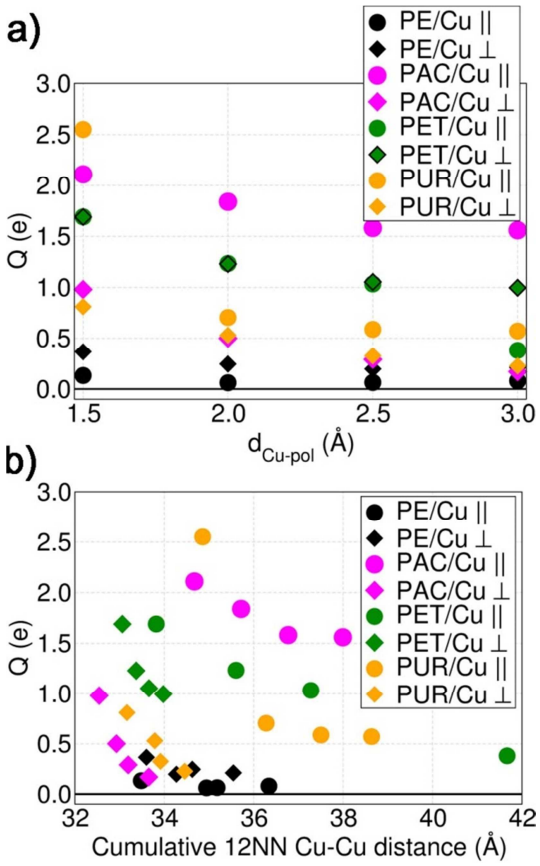

Figure 6. a) Computed Cu→polymer Bader charge transferred (Q, e) as a function of **a)** $d_{Cu\text{-}pol}$, and **b)** the average cumulative 12 NN Cu-Cu distance in the optimized Cu-polymer interface models.

3.2.3 Magnetic properties of the interface models

We find the relaxed Cu-polymer interfaces to be characterized by generally smaller band splitting (ΔE) and magnetic moments (m) with respect to bulk FCC Cu (Figure S6 in the Supporting Information). The direct (inverse) contribution of these parameters to the approximated Stoner exchange integral (I_S, Eq. 1) leads to scattering of the computed Cu-resolved I_S both above and below the bulk FCC Cu value, with largest values in the 1.1-1.3 eV range for all the different polymer considered, close and in cases above the largest value computed for as deposited ferromagnetic Cu-aC systems (I_S=1.25 eV).[31] In line with results for Cu-C_{60} interfaces,[30] the increase in I_S is not localized at the immediate Cu-polymer interface but spread over the whole Cu-substrate (Fig. S6 in the Supporting Information). Contrary to results for Cu-C_{60} hybrids,[30] but in

agreement with simulations of the Cu-aC interfaces,[31] no immediate correlation is found between the increase in I_S and the loosening of the Cu lattice as measured by the sum of the 12 NN Cu-Cu distances in the optimized slabs (Figure S7 in the Supporting Information).

In general, Cu-substrate averaged I_s values turn out to be either minimally larger (less than 0.1 eV increase) or smaller than for bulk FCC Cu (Figure 7a). An exception to this trend is the parallel Cu-PE interface with $d_{Cu\text{-}pol}$=2.0 Å. For this system the average I_S value is nearly 0.2 eV higher than bulk FCC Cu, first revealing that, pending favorable interface relaxation, significant increase in I_S can be also produced by interfacing Cu with non π-conjugated organics such as PE. The non-monotonic, system-dependent change of the computed I_S as a function of $d_{Cu\text{-}pol}$ (Fig. 7a) clearly indicates that relaxation of the interface under different geometrical constraints, as expected for Cu-samples of different crystallinity and homogeneity, can majorly affect the interfacial magnetic properties, answering one of the research questions behind the choice of the models.

With the exception of the in-plane (||) Cu-PAC ($d_{Cu\text{-}pol}$=2.0 Å and $d_{Cu\text{-}pol}$=2.5 Å) and Cu-PUR ($d_{Cu\text{-}pol}$=3.0 Å) systems, all the other interfaces result in a substantial increase (from over 20% to up to a factor of two) of the computed DOS(E_F) with respect to the bulk FCC value (Figure 7b). Notably, among the in-plane models, the largest DOS(E_F) values are computed for Cu interfaced with PE, that completely lacks π-conjugation. These results clearly demonstrate that the presence of a π-system, and ensuing enhancement of the Cu→organics charge-transfer (Figure 6) is not strictly necessary for enhancing the interfacial DOS(E_F): suitable interface relaxation and composition can also be effective to this end. It thus emerges that I_S and DOS(E_F), key quantities of the Stoner model of ferromagnetism,[52-53] are i) differently sensitive to the composition and structure of the interface, and ii) not directly correlated at least for the systems considered (see also Figure S8 in the Supporting Information).

Notably, in spite of the reduced interface relaxation (Figure 4) and charge-transfer (Figure 6), the computed DOS(E_F) for the perpendicular (⊥) interface models turns out to be comparable (or

noticeable larger in the case of PAC) with the value obtained for the in-plane (||) systems. It thus turns out that substantial increase of DOS(E_F) can be achieved also by relatively localized contacts between the Cu-substrate and the organic.

As shown in Figure 7c, the combination of the differently altered I_S and DOS(E_F) leads to I_S×DOS(E_F) products generally larger than for bulk FCC Cu, indicative of magnetic hardening. The only exception to trend is represented by the in-plane interface between Cu and PAC, the system with the most extended π-conjugated system and the largest Cu→organic charge-transfer (Figure 6). Further evidence of the non-immediate correlation between interface magnetic hardening and charge-transfer is provided by the fact that the I_S×DOS(E_F) products for the Cu-PE interface are comparable to those for π-conjugated polymers such as PET and PUR, in spite of the substantially different interfacial charge-transfer (Figure 6).

Contrary to what found in Ref. [30] for Cu-C_{60} interfaces, the largest computed I_S×DOS(E_F) does not appear to correlate with increased loosening of the Cu-lattice as measured by the cumulative 12 NN Cu-Cu distance (Figure 7d). Additionally, for the Cu-PUR interface, the computed I_s×DOS(E_F) is found to actually decrease as the Cu lattice is loosened.

Perhaps surprisingly, due to the simultaneous increase in both I_S (Figure 7a) and DOS(E_F) (Figure 7b) the in-plane Cu-PE interface for $d_{Cu\text{-}pol}$=2.0 Å is found to lead to the largest I_S×DOS(E_F) product (0.21 $spin^{-1}$ $atom^{-1}$), larger than what computed at the same level of theory for the annealed Cu-aC interface (0.19 $spin^{-1}$ $atom^{-1}$) measured to be ferromagnetic in Ref. [31]. Non-collinear fixed-spin DFT simulations of this Cu-PE interface points out minimal changes (<10^{-7} eV/atom) in the computed MAEs, that remain consistently in the order of 10^{-6} eV/atom, in line with the weak shape anisotropies measured for ferromagnetic Cu-C_{60} interfaces (~10^{-6} eV/Cu-atom).[30] The same considerations as for the sub-meV MAEs computed for bulk FCC Cu (Section 3.1) apply also here.

It thus transpires that, in spite of the negligible charge-transfer (Figure 6), the PE chain is nevertheless capable, via interface relaxation and the ensuing re-hybridization with the metal

(Figures S4 and S5 in the Supporting Information), of inducing magnetic hardening of Cu competitive to that observed for interfaces with substantially larger electron-depletion of Cu. Analysis of the computed Cu-resolved I_S values as a function of the atomic Bader charges (Figure S9 in the Supporting Information) rules out any direct correlation between atomic charges on Cu atoms and ensuing magnetic hardness as quantified by the I_S parameter, strengthening the conclusion that rather than charge-transfer, it is the Cu-organic re-hybridization to be crucial for the interface magnetic hardening. As the data for the Cu-PE interface (Figure 6) and published result for alkanes on transition metals[20, 54] indicate, important interfacial re-hybridization, leading to emergence of interface electronic states of desirable properties [in the present case an increased $I_S \times DOS(E_F)$ product due to joint or separate enhancement of I_S and $DOS(E_F)$], may take place also without substantial net charge-transfer between the metal and the organic. The computed strong magnetic hardening for the planar ($d_{Cu\text{-}pol}$=2.0 Å) and perpendicular ($d_{Cu\text{-}pol}$=3.0 Å) Cu-PE interface models in Figure 7d, together with the presence of empty "surface" states (amenable to PBE simulation[46] as done here) with a typical vacuum decay length of 3.0 Å for periodic PE chains,[46, 58] altogether suggest that re-hybridization of molecular (empty) surface states with a metal can also be effective in tuning the interface magnetic properties.

These results, if not contrast, at least significantly add to existing suggestions that charge-transfer from the metal to the π-conjugated molecule is necessary for magnetic hardening and the emergence of ferromagnetic ordering at Cu-organics interfaces.[30-32] Although results about the unnecessity of π-conjugation for the creation of highly spin-polarized states at the interface between a ferromagnetic metal and an organic molecule have been previously published,[20] to the best of our knowledge, here we provide the very first insights into i) negligible magnetic hardening at the interface between Cu and a completely π-conjugated substrate (PAC), and ii) the possibility of magnetic hardening at the interface between a transition metal and a non π-conjugated molecule. The comparable magnetic hardening between the Cu-aC (measured to be ferromagnetic in Ref. [31])

and Cu-PE interfaces prompts further research in the overlooked possibilities offered by (non π-conjugated) aliphatic molecules for promoting emergent magnetism at metal-organic interfaces.

The computed decrease in Cu magnetic hardening going from C_{60} to aC, [30-32] to the π-conjugated polymers considered here inevitably raises the question as to whether optimal re-hybridization between Cu and π-conjugated organics towards enhancement of interfacial magnetism requires fine-tuning of the strain of the π-system on the organics. We hope these results will stimulate further experimental and computational research into this aspect.

Finally, the computed substantial increase of the $I_S \times DOS(E_F)$ products for discontinuous contact between the organic and the Cu, as present in the perpendicular (⊥) PE and PAC interfaces prepared with $d_{Cu\text{-}pol} \geq 2.5$ Å in Figure 7c, is also worth of mention. The results for these systems suggest that, depending on the nature of the organic, non-homogenous interfaces (as in the perpendicular models) may also be effective in inducing interface re-hybridization and emergence of magnetic hardening, opening up for the study of less regular or more complex multi-layer depositions than pursued so far.[30-31]

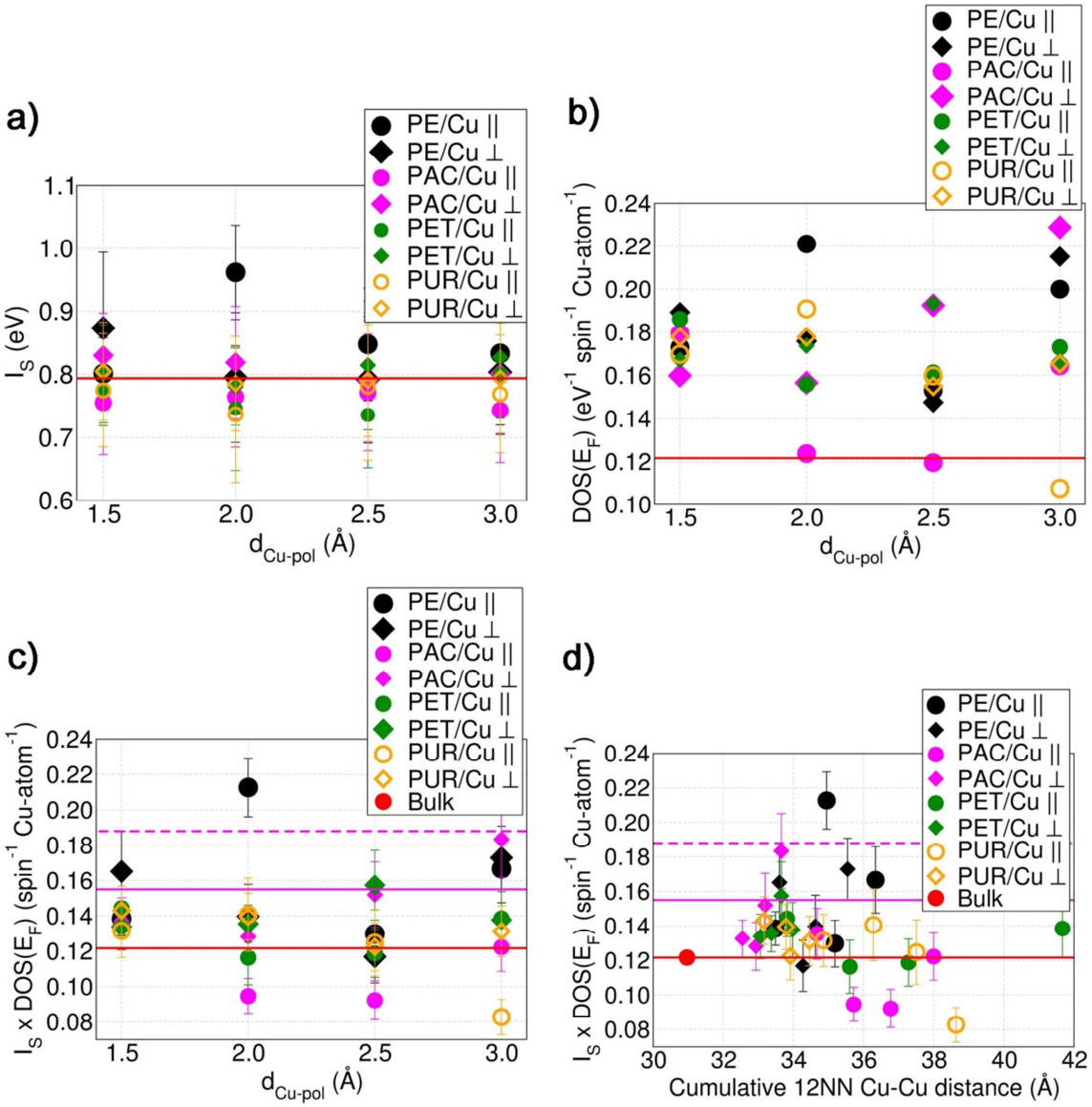

Figure 7. Average **a)** Stoner exchange integral (I_S), **b)** Density of States at the Fermi level [DOS(E_F)] and **c)** I_S×DOS(E_F) product for the Cu-polymer interface models as a function of $d_{Cu\text{-}pol}$. **d)** Average I_S×DOS(E_F) product as a function of the average cumulative 12 NN Cu-Cu distance in the optimized models. The horizontal red line marks the values for optimized bulk FCC Cu. The horizontal continuous (0.15 $spin^{-1}$ $atom^{-1}$) and dashed (0.19 $spin^{-1}$ $atom^{-1}$) magenta lines in c)-d) mark the largest computed I_S×DOS(E_F) product at the same level of theory for interfaces between Cu and as deposited (1.7 gr/cm^3) and annealed (2.3 gr/cm^3) aC measured to be ferromagnetic in Ref. [31].

4. CONCLUSION

In summary, DFT simulations have been used to investigate the role of lattice expansion and molecular π-conjugation for the magnetic hardening of Cu-organics interfaces. Analysis of the simulations for bare bulk FCC Cu and several models of the interfaces between Cu and differently π-conjugated polymers, namely polyethylene **(PE)**, polyacetylene **(PAC)**, polyethylene terephthalate **(PET)** and polyurethane **(PUR)** indicate that:

i) even in the absence of charge-transfer, 10-15% expansion of the bulk FCC Cu lattice results in magnetic hardening comparable to what computed for the interfaces between Cu and amorphous carbon measured to develop room-temperature ferromagnetic ordering.[31] Conversely, compression of the bulk FCC Cu lattice leads to magnetic softening of the metal.

ii) In spite of the substantially different, polymer-dependent, geometry relaxation, all the interfaces studied lead to metallization of the organic system.

iii) Organics with larger vertical electron affinity (EA) leads to larger charge-transfer when interfaced with Cu. This result suggests a secondary role for the interface relaxation and, pending further validation on a more extended set of systems, that the EA of the isolated molecule may be conveniently used in designing of charge-transfer at Cu-organics interfaces. The Cu→organic charge-transfer is found to be consistently suppressed by increase in the interfacial relaxation or loosening of the Cu lattice.

iv) At least for the systems studied, charge-transfer is found *not* to directly correlate with the interfacial magnetic hardening. The system with the most extended π-conjugation and largest interfacial charge-transfer (PAC) leads to the smallest magnetic hardening. Magnetic hardening appears to be governed by the details of the electronic re-hybridization with the metal. The precise role of strain in the π-system of the organic for such re-hybridization remains to be quantified.

v) Depending on the interfacial relaxation, re-hybridization between Cu and vacuum decaying empty states of the organic, as present in PE, are found to be effective in inducing interfacial magnetic hardening comparable with or larger than Cu-amorphous carbon systems recently measured to develop room-temperature ferromagnetic ordering.[31]

It thus transpires the neither the presence of the organic interface, molecular π-conjugation nor substantial charge-transfer may be strictly needed for magnetic hardening of Cu-substrates, albeit combination of the present results and available experimental data suggests that maximization of the effect does require both (strained) π-conjugation and substantial charge-transfer.[30-31] We believe these results prompts for further research in the, to date overlooked, possibilities of non π-conjugated molecules with empty surface states and maximally strained π-systems for magnetic hardening and emergent magnetism at transition-metal-organic interfaces.

ASSOCIATED CONTENT

Supporting Information. Supplementary DFT results and characterization. This is available free of charge via the Internet at http://pubs.acs.org

AUTHOR INFORMATION

Corresponding author

*E-mail: g.teobaldi@liv.ac.uk

ORCID

Dmitry G. Shchukin: 0000-0002-2936-804x

Gilberto Teobaldi: 0000-0001-6068-6786

Notes

The authors declare no competing financial interest.

ACKNOWLEDGMENTS

G.T. acknowledges support from EPSRC UK (EP/I004483/1, EP/K013610/1 and EP/P022189/1). D.G.S. acknowledges ERC (project ENERCAPSULE, Grant No. 647969). This work made use of the N8 (EPSRC UK EP/K000225/1), ARCHER (via the UKCP Consortium, EPSRC UK EP/K013610/1 and EP/P022189/1), and STFC Hartree Centre (Daresbury Laboratory, UK) High-Performance Computing facilities. G. T. is grateful to Oscar Céspedes for useful discussion and comments on the manuscript.

REFERENCES

1. Joachim, G.; Gimzewski, J.; Aviram, A., Electronics Using Hybrid-Molecular and Mono-Molecular Devices. *Nature* **2000**, *408*, 541.
2. Dimitrakopoulos, C. D.; Malenfant, P. R., Organic Thin Film Transistors for Large Area Electronics. *Adv. Mater.* **2002**, *14*, 99-117.
3. Sundar, V. C.; Zaumseil, J.; Podzorov, V.; Menard, E.; Willett, R. L.; Someya, T.; Gershenson, M. E.; Rogers, J. A., Elastomeric Transistor Stamps: Reversible Probing of Charge Transport in Organic Crystals. *Science* **2004**, *303*, 1644-1646.
4. Elbing, M.; Ochs, R.; Koentopp, M.; Fischer, M.; von Hänisch, C.; Weigend, F.; Evers, F.; Weber, H. B.; Mayor, M., A Single-Molecule Diode. *PNAS* **2005**, *102*, 8815-8820.
5. Oleynik, I.; Kozhushner, M.; Posvyanskii, V.; Yu, L., Rectification Mechanism in Diblock Oligomer Molecular Diodes. *Phys. Rev. Lett.* **2006**, *96*, 096803.
6. Díez-Pérez, I.; Hihath, J.; Lee, Y.; Yu, L.; Adamska, L.; Kozhushner, M. A.; Oleynik, I. I.; Tao, N., Rectification and Stability of a Single Molecular Diode with Controlled Orientation. *Nat. Chem.* **2009**, *1*, 635-641.
7. Céspedes, O.; Ferreira, M.; Sanvito, S.; Kociak, M.; Coey, J., Contact Induced Magnetism in Carbon Nanotubes. *J. Phys.: Condens. Matter* **2004**, *16*, L155.
8. Barraud, C.; Seneor, P.; Mattana, R.; Fusil, S.; Bouzehouane, K.; Deranlot, C.; Graziosi, P.; Hueso, L.; Bergenti, I.; Dediu, V., Unravelling the Role of the Interface for Spin Injection into Organic Semiconductors. *Nat. Phys.* **2010**, *6*, 615-620.
9. Schulz, L.; Nuccio, L.; Willis, M.; Desai, P.; Shakya, P.; Kreouzis, T.; Malik, V. K.; Bernhard, C.; Pratt, F.; Morley, N., Engineering Spin Propagation across a Hybrid Organic/Inorganic Interface Using a Polar Layer. *Nat. Mater.* **2011**, *10*, 39.
10. Sanvito, S., Molecular Spintronics. *Chem. Soc. Rev.* **2011**, *40*, 3336-3355.
11. Raman, K. V.; Kamerbeek, A. M.; Mukherjee, A.; Atodiresei, N.; Sen, T. K.; Lazic, P.; Caciuc, V.; Michel, R.; Stalke, D.; Mandal, S. K., Interface-Engineered Templates for Molecular Spin Memory Devices. *Nature* **2013**, *493*, 509.
12. Warner, M.; Din, S.; Tupitsyn, I. S.; Morley, G. W.; Stoneham, A. M.; Gardener, J. A.; Wu, Z.; Fisher, A. J.; Heutz, S.; Kay, C. W., Potential for Spin-Based Information Processing in a Thin-Film Molecular Semiconductor. *Nature* **2013**, *503*, 504.
13. Callsen, M.; Caciuc, V.; Kiselev, N.; Atodiresei, N.; Blügel, S., Magnetic Hardening Induced by Nonmagnetic Organic Molecules. *Phys. Rev. Lett.* **2013**, *111*, 106805.
14. Atodiresei, N.; Raman, K. V., Interface-Assisted Spintronics: Tailoring at the Molecular Scale. *MRS Bull.* **2014**, *39*, 596-601.
15. Moodera, J. S.; Koopmans, B.; Oppeneer, P. M., On the Path toward Organic Spintronics. *MRS Bull.* **2014**, *39*, 578-581.

16. Moorsom, T.; Wheeler, M.; Khan, T. M.; Al Ma'Mari, F.; Kinane, C.; Langridge, S.; Bedoya-Pinto, A.; Hueso, L.; Teobaldi, G.; Lazarov, V. K., Spin-Polarized Electron Transfer in Ferromagnet/C 60 Interfaces. *Phys. Rev. B* **2014**, *90*, 125311.
17. Bairagi, K.; Bellec, A.; Repain, V.; Chacon, C.; Girard, Y.; Garreau, Y.; Lagoute, J.; Rousset, S.; Breitwieser, R.; Hu, Y.-C., Tuning the Magnetic Anisotropy at a Molecule-Metal Interface. *Phys. Rev. Lett.* **2015**, *114*, 247203.
18. Gruber, M.; Ibrahim, F.; Boukari, S.; Isshiki, H.; Joly, L.; Peter, M.; Studniarek, M.; Da Costa, V.; Jabbar, H.; Davesne, V., Exchange Bias and Room-Temperature Magnetic Order in Molecular Layers. *Nat. Mater.* **2015**, *14*, 981-984.
19. Gruber, M.; Ibrahim, F.; Boukari, S.; Joly, L.; Da Costa, V.; Studniarek, M.; Peter, M.; Isshiki, H.; Jabbar, H.; Davesne, V., Spin-Dependent Hybridization between Molecule and Metal at Room Temperature through Interlayer Exchange Coupling. *Nano Lett.* **2015**, *15*, 7921-7926.
20. Djeghloul, F.; Gruber, M.; Urbain, E.; Xenioti, D.; Joly, L.; Boukari, S.; Arabski, J.; Bulou, H.; Scheurer, F.; Bertran, F. o., High Spin Polarization at Ferromagnetic Metal–Organic Interfaces: A Generic Property. *J. Phys. Chem. Lett.* **2016**, *7*, 2310-2315.
21. Heß, V.; Friedrich, R.; Matthes, F.; Caciuc, V.; Atodiresei, N.; Bürgler, D. E.; Blügel, S.; Schneider, C. M., Magnetic Subunits within a Single Molecule-Surface Hybrid. *New J. Phys.* **2017**.
22. Esat, T.; Friedrich, R.; Matthes, F.; Caciuc, V.; Atodiresei, N.; Blügel, S.; Bürgler, D. E.; Tautz, F. S.; Schneider, C. M., Quantum Interference Effects in Molecular Spin Hybrids. *Phys. Rev. B* **2017**, *95*, 094409.
23. Ibañez-Azpiroz, J.; Dias, M.; Schweflinghaus, B.; Blüegel, S.; Lounis, S., Tuning Paramagnetic Spin-Excitations of Single Adatoms. *Phys. Rev. Lett.* **2017**.
24. Cinchetti, M.; Dediu, V. A.; Hueso, L. E., Activating the Molecular Spinterface. *Nat. Mater.* **2017**, *16*, 507-515.
25. Carmeli, I.; Leitus, G.; Naaman, R.; Reich, S.; Vager, Z., Magnetism Induced by the Organization of Self-Assembled Monolayers. *J. Chem. Phys* **2003**, *118*, 10372-10375.
26. Vager, Z.; Naaman, R., Bosons as the Origin for Giant Magnetic Properties of Organic Monolayers. *Phys. Rev. Lett.* **2004**, *92*, 087205.
27. Crespo, P.; Litrán, R.; Rojas, T.; Multigner, M.; De la Fuente, J.; Sánchez-López, J.; García, M.; Hernando, A.; Penadés, S.; Fernández, A., Permanent Magnetism, Magnetic Anisotropy, and Hysteresis of Thiol-Capped Gold Nanoparticles. *Phys. Rev. Lett.* **2004**, *93*, 087204.
28. Hernando, A.; Crespo, P.; Garcia, M., Origin of Orbital Ferromagnetism and Giant Magnetic Anisotropy at the Nanoscale. *Phys. Rev. Lett.* **2006**, *96*, 057206.
29. Naaman, R.; Vager, Z., Cooperative Electronic and Magnetic Properties of Self-Assembled Monolayers. *MRS Bull.* **2010**, *35*, 429-434.
30. Al Ma'Mari, F.; Moorsom, T.; Teobaldi, G.; Deacon, W.; Prokscha, T.; Luetkens, H.; Lee, S.; Sterbinsky, G. E.; Arena, D. A.; MacLaren, D. A., Beating the Stoner Criterion Using Molecular Interfaces. *Nature* **2015**, *524*, 69-73.
31. Al Ma'Mari, F.; Rogers, M.; Alghamdi, S.; Moorsom, T.; Lee, S.; Prokscha, T.; Luetkens, H.; Valvidares, M.; Teobaldi, G.; Flokstra, M., Emergent Magnetism at Transition-Metal–Nanocarbon Interfaces. *PNAS* **2017**, *114*, 5583-5588.
32. Raman, K. V.; Moodera, J. S., Materials Chemistry: A Magnetic Facelift for Non-Magnetic Metals. *Nature* **2015**, *524*, 42-43.
33. Schwarz, K.; Mohn, P., Itinerant Metamagnetism in Yco2. *J. Phys. F: Met. Phys.* **1984**, *14*, L129.
34. Grimme, S.; Antony, J.; Ehrlich, S.; Krieg, H., A Consistent and Accurate Ab Initio Parametrization of Density Functional Dispersion Correction (Dft-D) for the 94 Elements H-Pu. *J. Chem. Phys* **2010**, *132*, 154104.
35. Kresse, G.; Furthmüller, J., Efficient Iterative Schemes for Ab Initio Total-Energy Calculations Using a Plane-Wave Basis Set. *Phys. Rev. B* **1996**, *54*, 11169.
36. Perdew, J. P.; Burke, K.; Ernzerhof, M., Generalized Gradient Approximation Made Simple. *Phys. Rev. Lett.* **1996**, *77*, 3865.
37. Methfessel, M.; Paxton, A., High-Precision Sampling for Brillouin-Zone Integration in Metals. *Phys. Rev. B* **1989**, *40*, 3616.
38. Henkelman, G.; Arnaldsson, A.; Jónsson, H., A Fast and Robust Algorithm for Bader Decomposition of Charge Density. *Comput. Mater. Sci.* **2006**, *36*, 354-360.

39. Gunnarsson, O., Band Model for Magnetism of Transition Metals in the Spin-Density-Functional Formalism. *J. Phys. F: Met. Phys.* **1976**, *6*, 587.
40. Lounis, S.; Costa, A.; Muniz, R.; Mills, D., Dynamical Magnetic Excitations of Nanostructures from First Principles. *Phys. Rev. Lett.* **2010**, *105*, 187205.
41. Lounis, S.; Costa, A.; Muniz, R.; Mills, D., Theory of Local Dynamical Magnetic Susceptibilities from the Korringa-Kohn-Rostoker Green Function Method. *Phys. Rev. B* **2011**, *83*, 035109.
42. Ueno, N.; Sugita, K.; Seki, K.; Inokuchi, H., Low-Energy Electron Transmission and Secondary-Electron Emission Experiments on Crystalline and Molten Long-Chain Alkanes. *Phys. Rev. B* **1986**, *34*, 6386.
43. Dudde, R.; Reihl, B., Complete Electronic Structure of Oriented Films of Hexatriacontane. *Chem. Phys. Lett.* **1992**, *196*, 91-96.
44. Bloor, D., Correlation of Experimental and Theoretical Electron Band Energies of Polyethylene. *Chem. Phys. Lett.* **1976**, *40*, 323-325.
45. Serra, S.; Tosatti, E.; Iarlori, S.; Scandolo, S.; Santoro, G., Interchain Electron States in Polyethylene. *Phys. Rev. B* **2000**, *62*, 4389.
46. Righi, M.; Scandolo, S.; Serra, S.; Iarlori, S.; Tosatti, E.; Santoro, G., Surface States and Negative Electron Affinity in Polyethylene. *Phys. Rev. Lett.* **2001**, *87*, 076802.
47. Demir, P.; Akman, F., Molecular Structure, Spectroscopic Characterization, Homo and Lumo Analysis of Pu and Pcl Grafted onto Pema-Co-Phema with Dft Quantum Chemical Calculations. *J. Mol. Struct.* **2017**, *1134*, 404-415.
48. Rajopadhye, N.; Bhoraskar, S., Ionization Potential and Work Function Measurements of Pp, Pet and Fep Using Low-Energy Electron Beam. *J. Mater. Sci. Lett.* **1986**, *5*, 603-605.
49. Horný, L. u.; Petraco, N. D.; Pak, C.; Schaefer, H. F., What Is the Nature of Polyacetylene Neutral and Anionic Chains Hc2 N H and Hc2 N H-(N= 6− 12) That Have Recently Been Observed? *JACS* **2002**, *124*, 5861-5864.
50. Dissado, L. A.; Fothergill, J. C., *Electrical Degradation and Breakdown in Polymers*; IET, 1992; Vol. 9.
51. Pai, W. W.; Jeng, H.; Cheng, C.-M.; Lin, C.-H.; Xiao, X.; Zhao, A.; Zhang, X.; Xu, G.; Shi, X.; Van Hove, M., Optimal Electron Doping of a C 60 Monolayer on Cu (111) Via Interface Reconstruction. *Phys. Rev. Lett.* **2010**, *104*, 036103.
52. Stoner, E. C., Collective Electron Ferromagnetism. *Proc. R. Soc. A* **1938**, 372-414.
53. Stoner, E. C., Collective Electron Ferromagnetism. Ii. Energy and Specific Heat. *Proc. R. Soc. A* **1939**, 339-371.
54. Öström, H.; Triguero, L.; Weiss, K.; Ogasawara, H.; Garnier, M.; Nordlund, D.; Nyberg, M.; Pettersson, L.; Nilsson, A., Orbital Rehybridization in N-Octane Adsorbed on Cu (110). *J. Chem. Phys* **2003**, *118*, 3782-3789.
55. Cubero, D.; Quirke, N.; Coker, D. F., Electronic Transport in Disordered N-Alkanes: From Fluid Methane to Amorphous Polyethylene. *J. Chem. Phys* **2003**, *119*, 2669-2679.
56. Cubero, D.; Quirke, N.; Coker, D. F., Electronic States for Excess Electrons in Polyethylene Compared to Long-Chain Alkanes. *Chem. Phys. Lett.* **2003**, *370*, 21-25.
57. Wang, Y.; MacKernan, D.; Cubero, D.; Coker, D. F.; Quirke, N., Single Electron States in Polyethylene. *J. Chem. Phys* **2014**, *140*, 154902.
58. Echenique, P.; Pendry, J., Theory of Image States at Metal Surfaces. *Prog. Surf. Sci.* **1989**, *32*, 111-159.

TABLE OF CONTENTS image

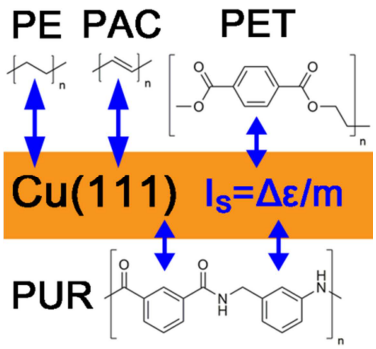

SUPPORTING INFORMATION

The Role of Metal Lattice Expansion and Molecular π-Conjugation for the Magnetic Hardening at Cu-Organics Interfaces

Lorena Martín-Olivera,[a] Dmitry Shchukin,[a] and Gilberto Teobaldi[a,b,*]

[a] *Stephenson Institute for Renewable Energy, Department of Chemistry, the University of Liverpool, L69 3BX Liverpool, United Kingdom*

[b] *Beijing Computational Science Research Centre, Beijing 100193, China*

* E-mail: g.teobali@liv.ac.uk

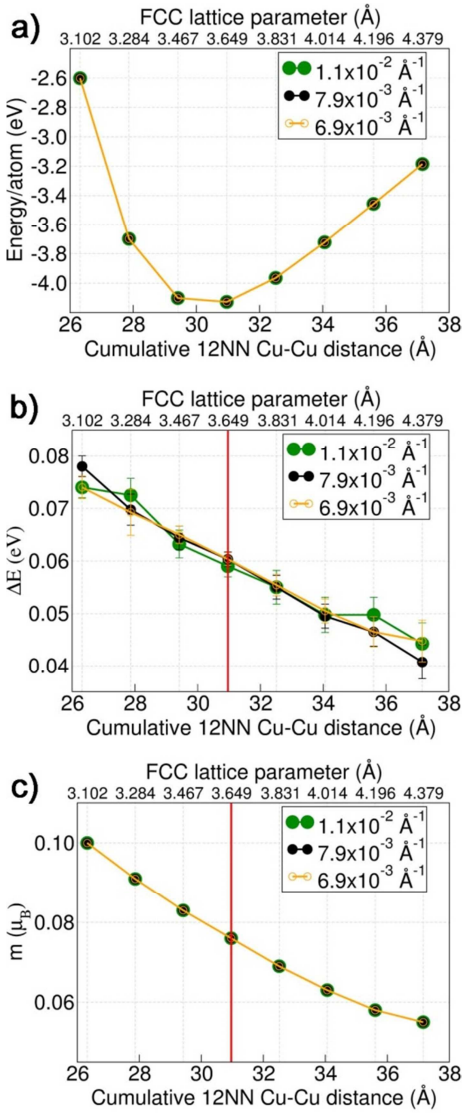

Figure S1. Computed **a)** energy per Cu-atom, **b)** band-splitting (ΔE), and **c)** atomic magnetic moment (m) as a function of the lattice parameter for bulk Cu in the face-centered cubic (FCC) structure for different k-point sampling. For each structure considered, the sum of the 12 shortest nearest-neighbours (NN) Cu-Cu distances is also indicated. The vertical red line marks the value of cumulative 12NN Cu-Cu distance (30.962 Å) in bulk FCC Cu for the optimized lattice parameter (3.649 Å).

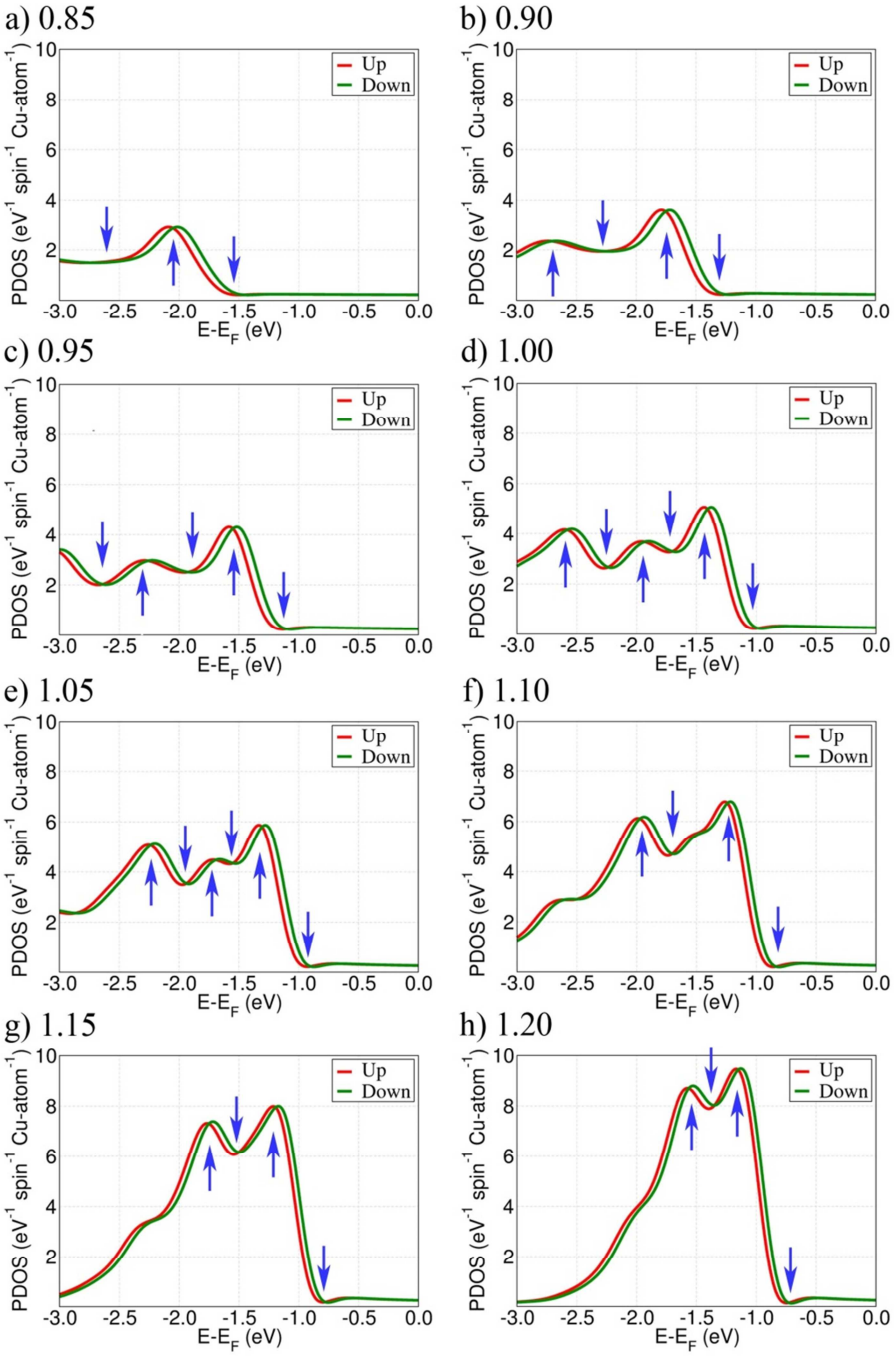

Figure S2. Spin-resolved Cu-projected PDOS for bulk FCC Cu isotropically deformed via scaling, by a factor of **a)** 0.85, **b)** 0.90, **c)** 0.95, **d)** 1.00, **e)** 1.05, **f)** 1.10, **g)** 1.15, **h)** 1.20, of the optimized lattice parameter. The blue arrows mark the stationary (maxima and minima) points used for the computation of the average I_S value and its standard deviation, taken as error of I_S.

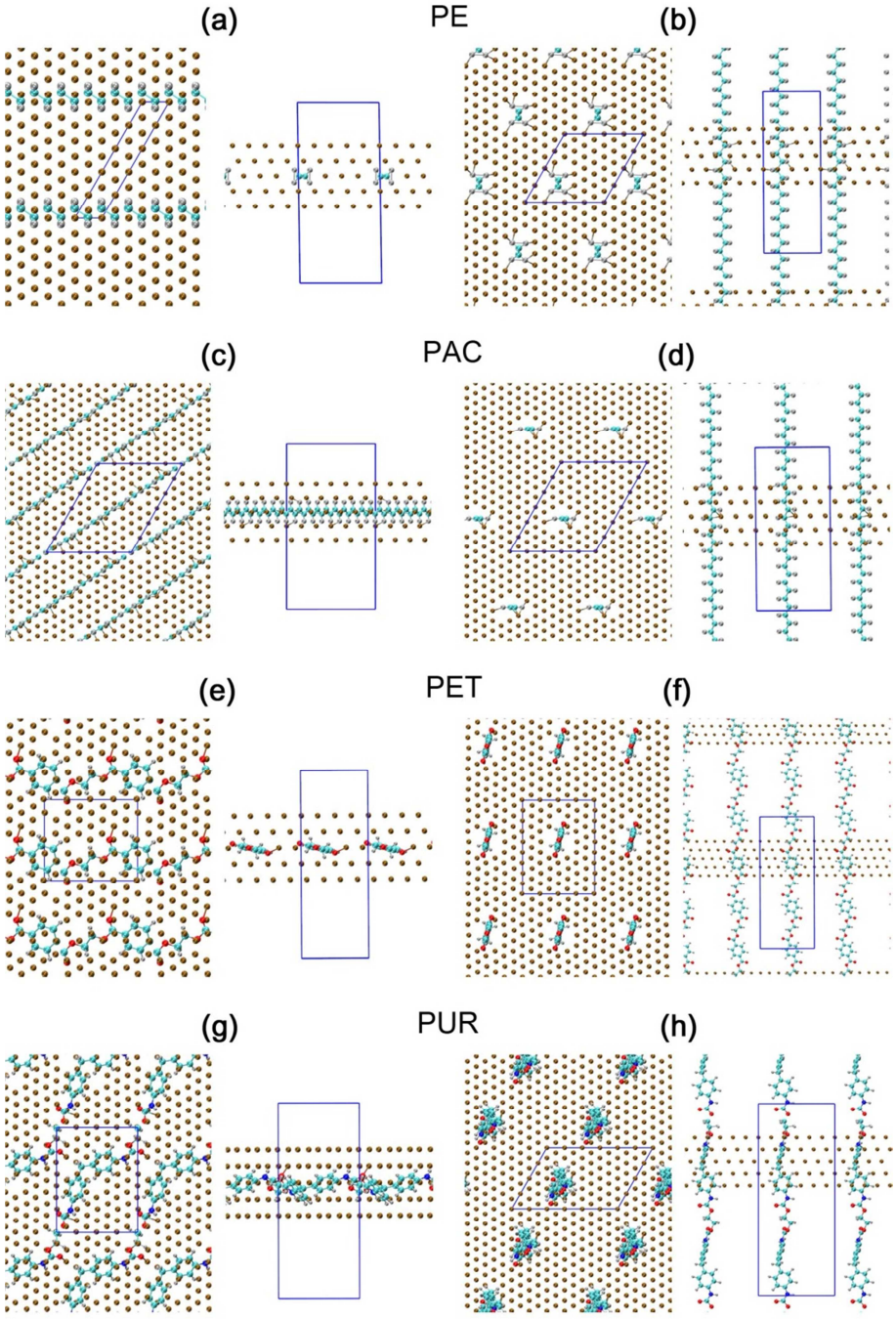

Figure S3. Top (left) and side (right) view of the initial geometries ($d_{Cu\text{-}pol}$=1.5 Å) for the in-plane (||) and perpendicular (⊥) models of the Cu interfaces with PE [**a)** || geometry, **b)** ⊥ geometry], PAC [**c)** || geometry, **d)** ⊥ geometry], PET [**e)** || geometry, **f)** ⊥ geometry] and PUR [**g)** || geometry, **h)** ⊥ geometry]. The periodic simulation cell is marked by blue continued lines. C: cyan, O: red, N: blue, H: silver, Cu: brown.

Table S1. Geometric parameters of the simulations cell for the different Cu(111)-polymer interface models studied. l_0 (Å): length of the monomer unit. N_p: number of monomer units in the Cu-polymer interface model. h: hexagonal cell. o: orthorhombic cell. The positive lattice mismatch values indicate that the polymer chain was stretched to match the Cu(111) slab one.

	l_0 (Å)	N_p	Model	Cu(111) super-cell	In-plane periodicity (Å^2)	Lattice mismatch (%)
PE	**2.55**	**1**	∥	$(1x5)_h$	**2.58x12.90**	**1.19**
		10	⊥	$(4x4)_h$	**10.32x10.32**	
PAC	**2.45**	**10**	∥	$(5x6)_h$	**12.90x15.48**	**0.46**
		10	⊥	$(5x6)_h$	**12.90x15.48**	
PET	**10.90**	**1**	∥	$(4x2)_o$	**10.32x8.94**	**3.09**
		3	⊥	$(3x4)_o$	**10.32x13.41**	
PUR	**16.90**	**1**	∥	$(3x4)_o$	**10.32x13.41**	**0.12**
		2	⊥	$(6x4)_h$	**15.48x10.32**	

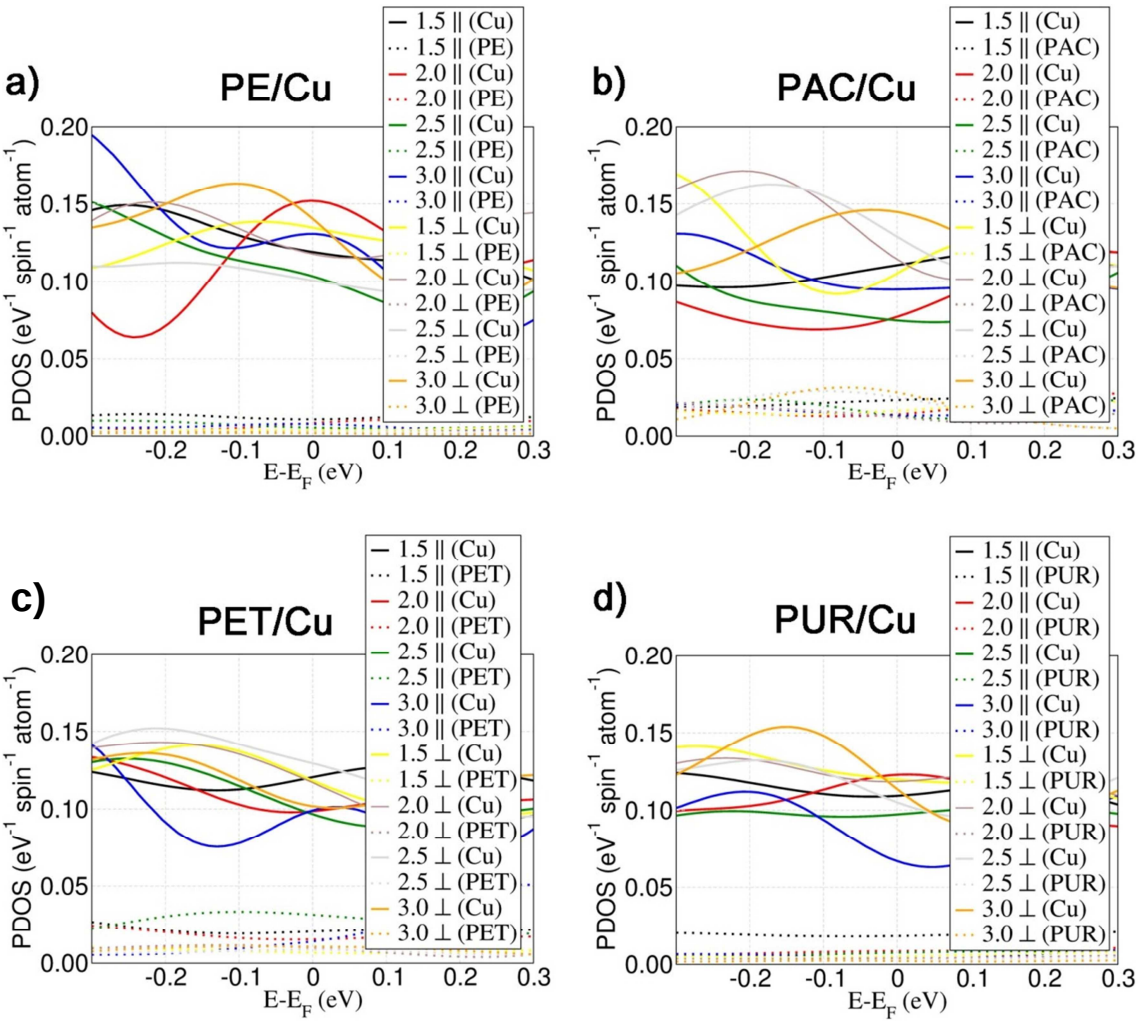

Figure S4. Cu (continuous) and organic (dotted) resolved atom-projected DOS (PDOS) for the models of the interface between Cu and **a)** PE, **b)** PAC, **c)** PET, **d)** PUR.

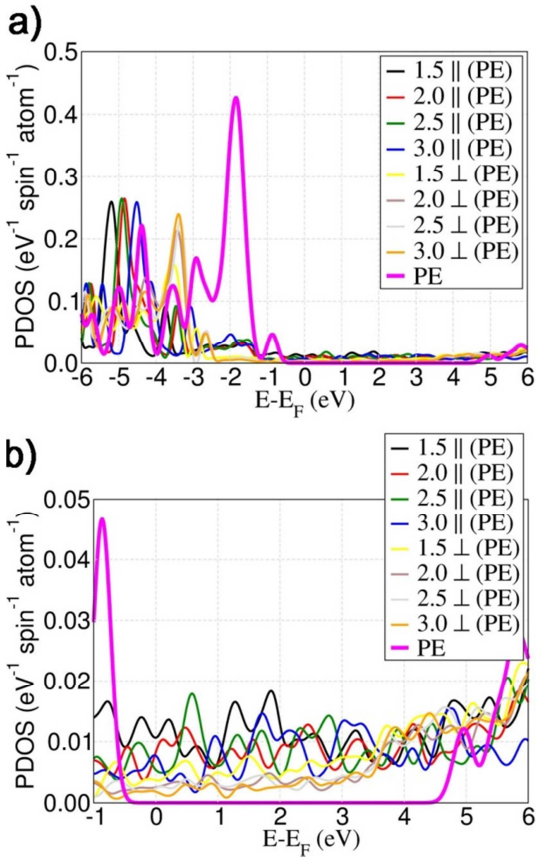

Figure S5. a) PE-resolved PDOS for one isolated PE chain (with a well-defined HOMO-LUMO gap) and the different Cu/PE interface models considered. **b)** Close up of the PDOS around the Fermi level (E-E_F=0 eV). In all cases, and regardless of the initial Cu-PE distance cut-off used to prepare the starting geometry, re-hybridization and metallization [non-zero PDOS(E_F)] of the PE interfaced to Cu is evident.

Table S2. Computed vacuum-aligned LUMO energy for the isolated chains of the polymer considered (at their optimized periodicity).

System	E_{LUMO} (eV)
PE	-0.85
PAC	-3.68
PET	-3.28
PUR	-1.68

Table S3. Average computed C-H (d_{CH}, Å), C-C (d_{CC}, Å) bond distances and C-C-C angles (θ_{CCC}, degrees) for PE in the Cu-PE interface models with standard deviation. Values for one isolated PE chain at the optimized periodicity are also reported for comparison.

		Average over all the PE atoms in the system		
Interface geometry	**Cut-off (Å)**	**d_{CC}**	**d_{CH}**	**θ_{CCC}**
∥	1.5	1.5186 ± 0.0003	1.1147 ± 0.0019	116.3281 ± 0.0001
	2.0	1.5242 ± 00001	1.1146 ± 0.0043	115.6526 ± 0.0001
	2.5	1.5217 ± 0.0002	1.1156 ± 0.0042	115.9453 ± 0.0001
	3.0	1.5266 ± 0.0002	1.1128 ± 0.0017	115.4468 ± 0.0001
⊥	1.5	1.5220 ± 0.0110	1.1131 ± 0.0098	114.4590 ± 1.916
	2.0	1.5240 ± 0.00733	1.1097 ± 0.0050	113.6498 ± 0.7368
	2.5	1.5229 ± 0.0094	1.1102 ± 0.0075	113.8548 ± 1.2708
	3.0	1.5254 ± 0.0072	1.1084 ± 0.0049	113.6875 ± 1.1376
		Average over all the PE atoms in the Cu-slab		
⊥	1.5	1.5110 ± 0.0110	1.1204 ± 0.0068	114.8883 ± 2.5008
	2.0	1.5148 ± 0.0056	1.1149 ± 0.0047	114.0937 ± 1.0184
	2.5	1.5123 ± 0.0086	1.1180 ± 0.0091	114.1678 ± 1.4085
	3.0	1.5128 ± 0.0068	1.1157 ± 0.0049	114.3301 ± 2.5238
		Isolated PE chain at the optimized periodicity		
		1.5274 ± 0.0001	1.1049 ± 0.0001	113.1819 ± 0.0001

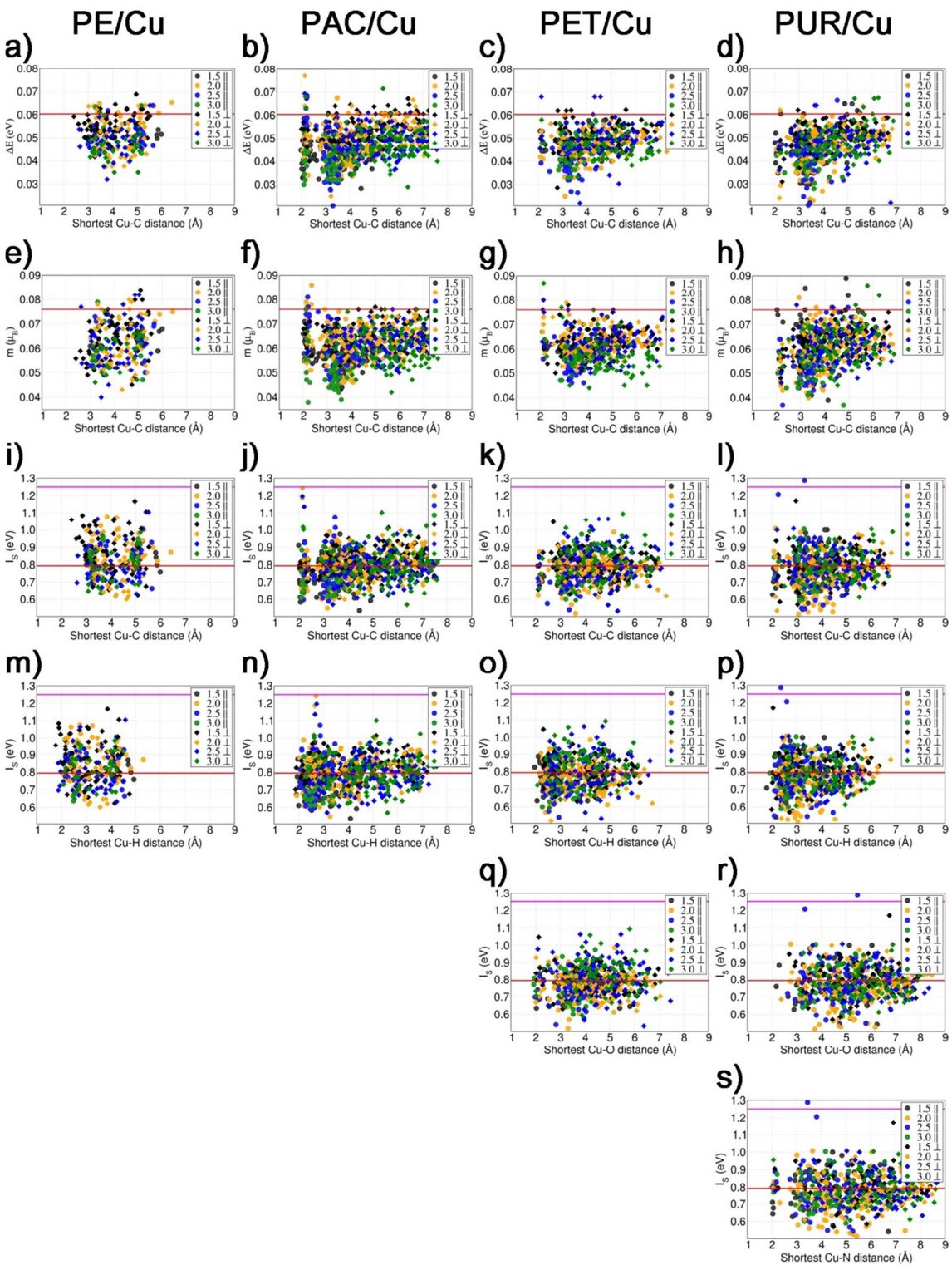

Figure S6. Cu-atom resolved band-splitting [ΔE, panels **a)** to **d)**], atomic magnetic moment [m, panels **e)** to **h)**] and Stoner exchange integral [I_S, panels **i)** to **s)**] for the Cu-polymer interface models studied as a function of the shortest Cu-C [panels **a)** to **l)**], Cu-H [panels **m)** to **p)**], Cu-O [panels **q)** to **r)**] and Cu-N [panel **s)**] distance. The horizontal red line marks the values for FCC bulk Cu at the optimized lattice parameter (3.649 Å). The horizontal continuous magenta line in panels (i-s) marks the maximum I_S value (1.25 eV) computed for the interface between Cu and as deposited (1.7 gr/cm^3) amorphous carbon, measured to be ferromagnetic in Ref. 31.

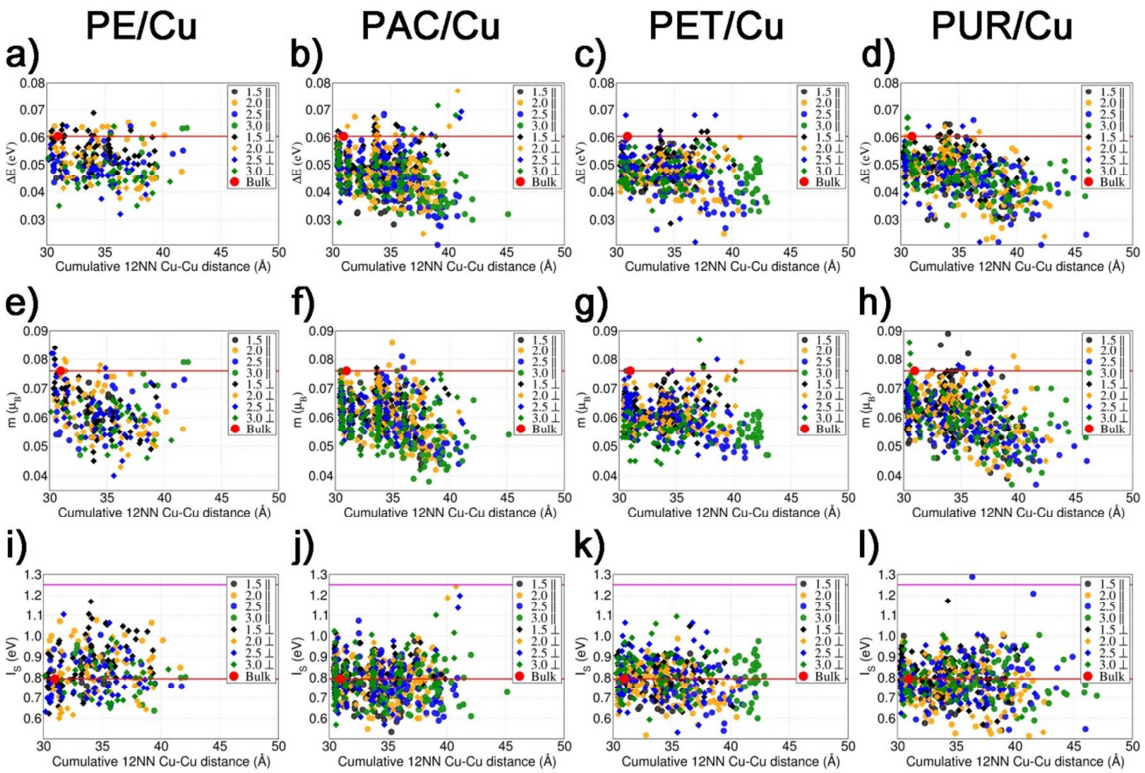

Figure S7. Cu-atom resolved band-splitting [ΔE, panels **a)** to **d)**], atomic magnetic moment [m, panels **e)** to **h)**] and Stoner exchange integral [I_S, panels **i)** to **l)**] for the Cu-polymer interface models studied as a function of the cumulative 12 NN Cu-Cu distances. The horizontal red line marks the values for FCC bulk Cu at the optimized lattice parameter (3.649 Å). The horizontal continuous magenta line in panels (i-l) marks the maximum I_S value (1.25 eV) computed for the interface between Cu and as deposited (1.7 gr/cm^3) amorphous carbon, measured to be ferromagnetic in Ref. 31.

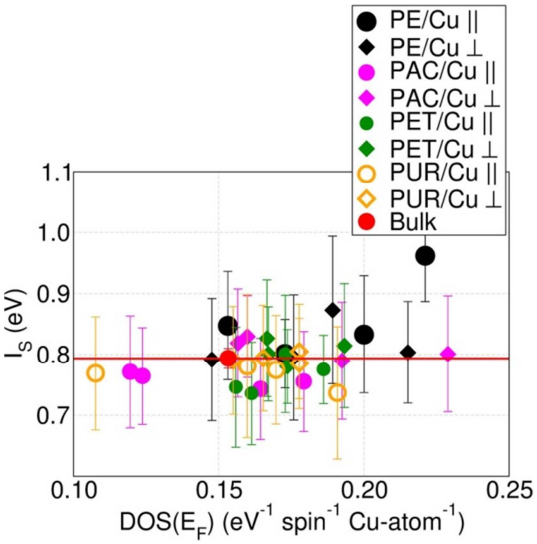

Figure S8. System-averaged I_S as a function of DOS(E_F) for the interface model considered. I_S and DOS(E_F) are evidently uncorrelated.

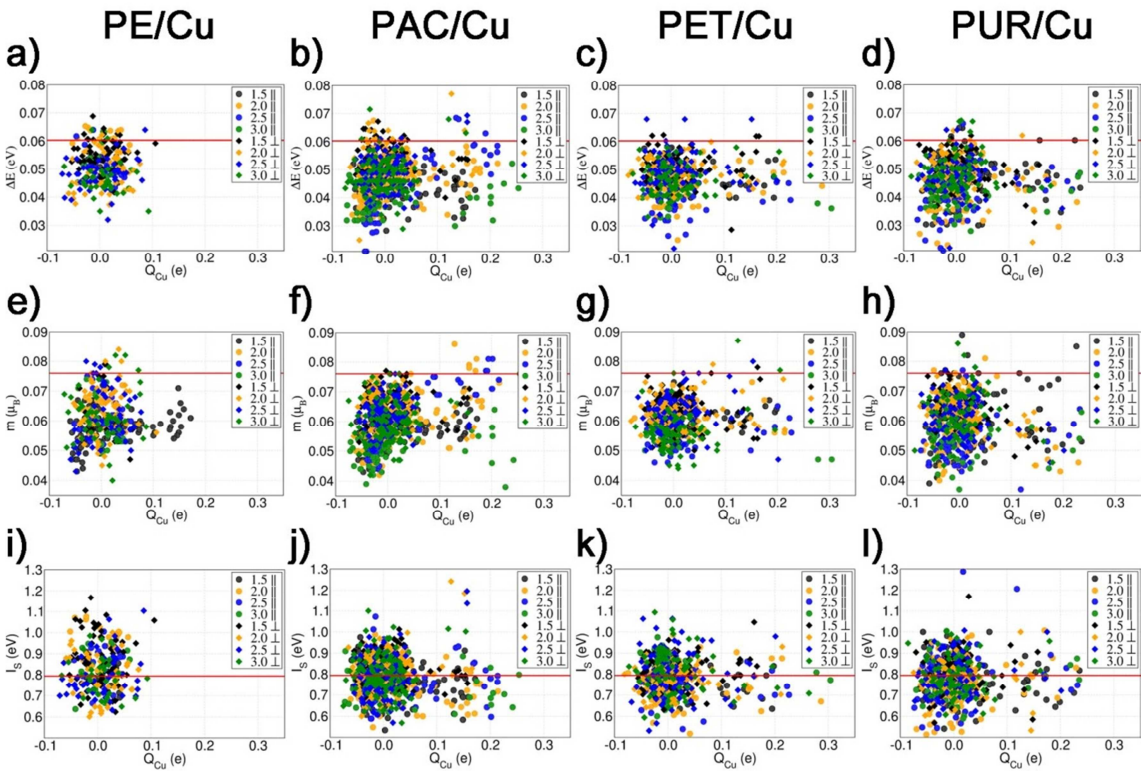

Figure S9. Cu-atom resolved band-splitting [ΔE, panels **a)** to **d)**], atomic magnetic moment [m, panels **e)** to **h)**] and Stoner exchange integral [I_S, panels **i)** to **l)**] for the Cu-polymer interface models studied as a function of the Cu atomic Bader charge. The horizontal red line marks the values for FCC bulk Cu at the optimized lattice parameter (3.649 Å). The horizontal continuous magenta line in panels (i-l) marks the maximum I_S value (1.25 eV) computed for the interface between Cu and as deposited (1.7 gr/cm^3) amorphous carbon, measured to be ferromagnetic in Ref. 31.